Annu. Rev. Biomed. Eng. 2000. 02:289–313

MICROFABRICATED MICRONEEDLES FOR GENE AND DRUG DELIVERY

Devin V. McAllister[1], Mark G. Allen[2], and Mark R. Prausnitz[1,3]

Schools of [1]Chemical Engineering, [2]Electrical and Computer Engineering, and [3]Biomedical Engineering, Georgia Institute of Technology, Atlanta, Georgia 30332; e-mail: gt3501b@prism.gatech.edu, mallen@ece.gatech.edu, mark.prausnitz@che.gatech.edu

Key Words micromachining, MEMS, injections, needles, DNA

■ **Abstract** By incorporating techniques adapted from the microelectronics industry, the field of microfabrication has allowed the creation of microneedles, which have the potential to improve existing biological-laboratory and medical devices and to enable novel devices for gene and drug delivery. Dense arrays of microneedles have been used to deliver DNA into cells. Many cells are treated at once, which is much more efficient than current microinjection techniques. Microneedles have also been used to deliver drugs into local regions of tissue. Microfabricated neural probes have delivered drugs into neural tissue while simultaneously stimulating and recording neuronal activity, and microneedles have been inserted into arterial vessel walls to deliver antirestenosis drugs. Finally, microhypodermic needles and microneedles for transdermal drug delivery have been developed to reduce needle insertion pain and tissue trauma and to provide controlled delivery across the skin. These needles have been shown to be robust enough to penetrate skin and dramatically increase skin permeability to macromolecules.

CONTENTS

1523-9829/00/0825-0289$14.00

INTRODUCTION

For over 150 years, syringes and hypodermic needles have been delivering drugs into patients. The hollow needle was invented in 1844, and the first injection was delivered shortly after (1). The practice of medicine has been revolutionized ever since. The needle's impact as a drug delivery vehicle is still strong today, partly because many pharmaceuticals are poorly absorbed in the intestine and/or sensitive to enzymatic degradation and thus cannot be administered orally.

Early syringes and needles were one piece and made of metal; the drug was injected via a leather plunger (2). These syringes were reused and difficult to sterilize. Today the syringe and hypodermic needle have evolved into a two-part disposable device. In current clinical practice, the syringe is typically made of plastic, and the needle is made of medical-grade stainless steel. Currently, the smallest needles available for injections are used largely for insulin administration, measuring 30 gauge for conventional syringes and 31 gauge for pen injectors. The 30- and 31-gauge needles have outer diameters of 305 μm and 254 μm, respectively (Becton Dickinson, Franklin Lakes, NJ).

Current research reviewed in this article has used microfabrication technology to shrink the needle, thereby improving existing devices or enabling novel devices for gene and drug delivery. Microfabrication [i.e. micromachining or microelectromechanical systems (MEMS)] uses tools developed by the microelectronics industry to make integrated circuits (ICs) and consists of a broad range of technologies anchored in the core technology of microlithographic pattern transfer (4–6). Microfabrication is an attractive approach because it can make small needles or microneedles, which can be used for local and/or painless delivery of compounds into cells or tissues. This technology also has the potential for cheap, highly reproducible batch fabrication of microneedles, which could be manufactured in combination with integrated circuits, micropumps, microsensors, and other microaccessories. Given all of these possible benefits, it is not surprising that there is widespread interest in microneedles, as indicated by the literature reviewed here and the extensive patent activity in the field (7–11).

Microfabrication is emerging as a global industry, unlike the microelectronics industry, which has been dominated by the United States and Japan (12). World-wide sales of MEMS-based devices are expected to grow from a range of \$2.8–\$4.7 billion in 1996 to \$12–\$20 billion in 2003. Five classes of devices have dominated the MEMS market: accelerometers (e.g. in airbags, pacemakers, and joysticks), hard disk drive heads (in computers), inkjet nozzles (in printers), microgyros (in braking systems and image stabilizers), and pressure sensors (in automobile engines and blood pressure monitors). Most of these devices

have found application in the automotive or information technology industries. However, microfabrication is projected to have a growing impact on biological applications.

The ability to fabricate microstructures or micromachines for biological applications is especially compelling because such devices can be made on the same size scale as the biological entity to be manipulated. Many different types of these devices are being pursued, such as DNA analysis chips (13–15), minimally invasive surgical tools (16–18), microstructures for studying cell properties and functions (19–21), microstructures that assist nerve regeneration (22), and controlled release of drugs from microchips (23), as reviewed elsewhere (24, 25). These devices can be divided into four categories based on their applications: (*a*) tools for molecular biology and biochemistry, (*b*) tools for cell biology, (*c*) medical devices, and (*d*) biosensors (25). The microneedles discussed here have the potential to affect all four of these categories.

We present progress in microneedle research for gene and drug delivery in the context of three broad applications: (*a*) cellular delivery, (*b*) local delivery, and (*c*) systemic delivery. As discussed below, microneedles can deliver molecules to cells in culture, into localized regions of tissue inside the body, and across the skin into the circulatory system. Some of these microneedle technologies are based on a more mature body of literature that concerns microfabricated electrode arrays used largely as neural probes (26–32). All microneedle technologies have their roots in microfabrication (4) and microelectronics fabrication (5, 6).

CELLULAR DELIVERY

The delivery of membrane-impermeable molecules into cells is needed for a broad variety of applications in molecular and cell biology. Molecules of interest include peptides, proteins, oligonucleotides, DNA, and a variety of other probes that alter or assay cell function. Currently available methods for introducing molecules into cells can be divided into four categories: chemical (e.g. ATP, EDTA, $CaPO_4$, or DEAE-dextran), vehicles (e.g. erythrocyte fusion or vesicle fusion), electrical (e.g. electroporation), and mechanical (e.g. microinjection, hyposmotic shock, sonication, or microprojectiles) (33, 34). These techniques either present the molecules in a way that causes them to be internalized by normal cellular functions or transiently disrupt the cell membrane to provide access to the cytosol. However, all of these methods have limitations, such as using cells or molecules with low efficiency, yielding impaired cell functions or cell death, requiring time and expertise, needing expensive equipment, and being applicable to only certain cell types and/or molecules.

In many ways, microinjection is the gold standard method for loading cells; it can reproducibly deliver large numbers of macromolecules to most cell types with high cell viability and function (33). However, because this technique involves injecting cells one at a time with individual glass micropipettes observed under

a microscope, it is extremely labor intensive and is practical only when treating small numbers of cells (e.g. <100 cells). To make microinjection simpler and faster, the research reviewed in this section on cellular delivery seeks to perform microinjection simultaneously on thousands of cells or more, with arrays of densely spaced microneedles (needle density can exceed $10^5/cm^2$). With multiple needles arranged in a high-density array, many cells can be treated at one time, which overcomes the major limitation of microinjection.

Silicon Microprobes for DNA Injection

To develop an efficient method for transforming cells, arrays of micromechanical piercing structures or microprobes were fabricated and successfully used to deliver genetic material into plant, nematode, and mammalian cells (35–37). The silicon microprobes (Figure 1) are pyramidal in shape and are solid (i.e. not hollow). Molecules to be delivered are either coated onto the microprobes before insertion into cells or the molecules are in solution around the cells when the microprobes are inserted.

The microprobes are bulk micromachined by a single-mask process that defines arrays of square silicon dioxide masks on a silicon wafer (35; Figure 2). The arrays of silicon dioxide squares are defined by standard photolithography techniques. First, photoresist (a photosensitive polymer) is spin cast onto a silicon dioxide-

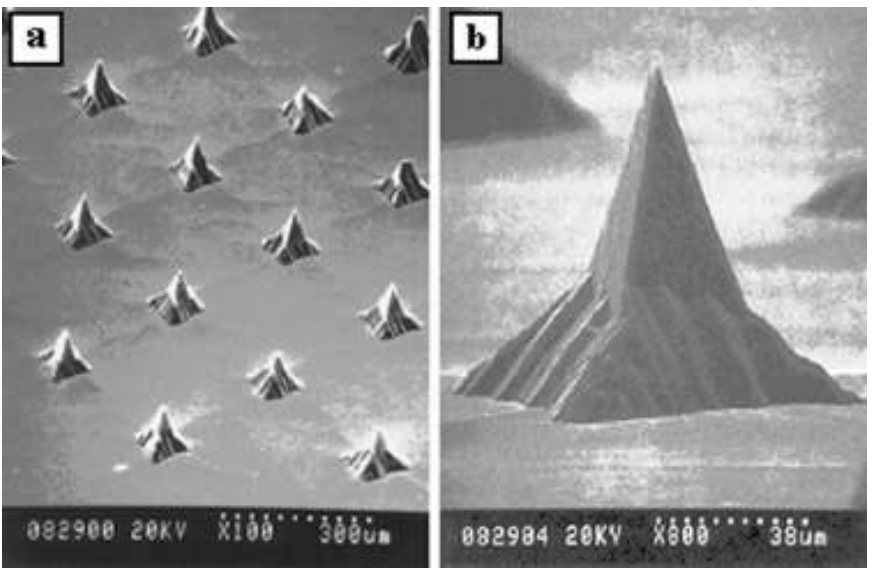

Figure 1 Scanning electron micrographs of (*a*) a silicon microprobe array and (*b*) a single microprobe used to deliver genes to plant, nematode, and mammalian cells and across vascular tissue. Reproduced with permission from Reference 36.

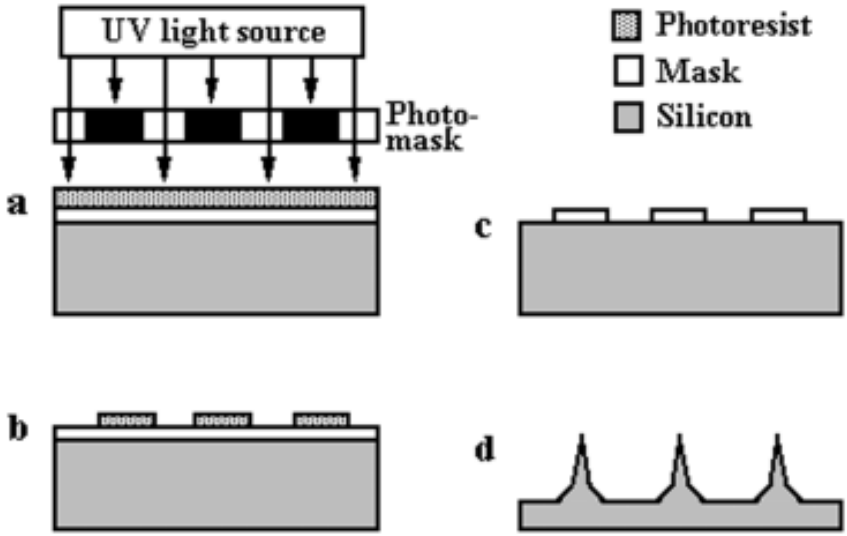

Figure 2 Microprobe or microneedle fabrication sequence. This process consists of (*a*) photodefining the photoresist by selective exposure to UV light through a photomask, (*b*) developing the photoresist, (*c*) etching the mask layer and removing the photoresist, and (*d*) performing an anisotropic etch to undercut the masks, leaving behind arrays of sharp microprobes or solid microneedles. This process yields microneedles shown in Figures 1 and 14*b* and *c*.

coated wafer. The wafer is then brought into contact with a photomask and exposed to UV light, which causes selective breakdown of the exposed polymer (Figure 2*a*). A photomask is generally a glass plate with a chromium pattern on it. The portions of the photoresist exposed to the UV light (i.e. not covered by the opaque chromium pattern) are removed during a subsequent development step (Figure 2*b*). This type of photoresist is referred to as a positive photoresist. The pattern thus transferred from the photomask to the photoresist is then etched into the silicon dioxide masking layer, and the photoresist is removed (Figure 2*c*). The wafer is then anisotropically wet etched in a solution of potassium hydroxide (38) until the silicon dioxide masks are undercut and fall off (Figure 2*d*).

This fabrication process leaves behind arrays of pyramid-shaped probes that can range in height from ten to several hundred micrometers and are extremely sharp (tip radii $<0.1\ \mu$m). This pyramidal structure arises because of the fast etch rate of the (411) crystalline planes of silicon in potassium hydroxide; the probes are therefore bounded by (411) planes.

These pyramidal microprobes have been used to deliver a plasmid vector pB121 into tobacco cells (*Nicotiana tabacum* W3). This plasmid vector contained a kanymycin resistance gene and a gene for β-glucuronidase. The tobacco cells, prepared by removing the epidermal layer of a tobacco leaf, were placed in a solution of DNA, and the microprobes were applied. Treated cells exhibited transient

expression of β-glucuronidase as indicated by the appearance of dark blue-green dots, whereas controls (microprobes without DNA or with DNA alone) did not (35).

These microprobes have also been used to deliver a plasmid vector containing a gene coding for β-galactosidase into the nematode *Caenorhabditis elegans*. Nematodes were pipetted onto microprobe arrays coated with DNA. The nematodes were then allowed to crawl off the arrays (thereby being pierced by the microprobes) and into culture medium. Of first generation hermaphrodite progeny, 8% exhibited the characteristic blue staining caused by β-galactosidase transfection, whereas the control group (microprobes without DNA or with DNA alone) did not show expression (35, 36). Microprobes coated with DNA have also transfected rat smooth muscle cells with a β-galactosidase gene by insertion into cell culture monolayers (37). Microprobe tips were not damaged during insertion into cells.

Glass Microcapillaries for DNA Injection

Arrays of hollow microcapillaries have been developed to achieve high-efficiency cell transformation as well as precise control over the amount of material delivered (39–41). These devices, which consist of an array of hollow silicon dioxide microcapillaries (Figure 3), have been used to inject both DNA and fluorescent dyes into plant cells. The microcapillaries are inserted into cells, and then molecules are delivered by injection through the lumen of the capillaries. By injecting the molecules through a well-defined lumen, precise amounts can be delivered into the cells.

The microcapillaries are bulk silicon micromachined by a single-mask process to define an array of circular holes in a silicon dioxide-masking layer on a silicon wafer (39–41; Figure 4). The arrays of holes are then etched deeply into the silicon

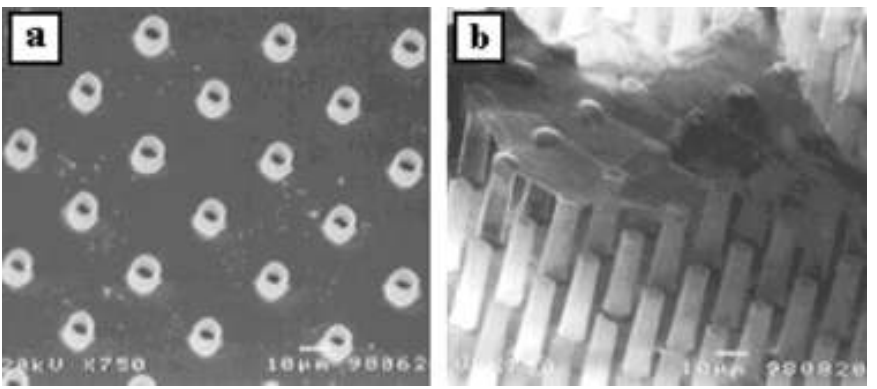

Figure 3 Scanning electron micrographs of (*a*) a section of an array of hollow microcapillaries and (*b*) microcapillaries covered with cellular debris. These microcapillaries are used to microinject DNA into many cells simultaneously. Reproduced with permission from Reference 39.

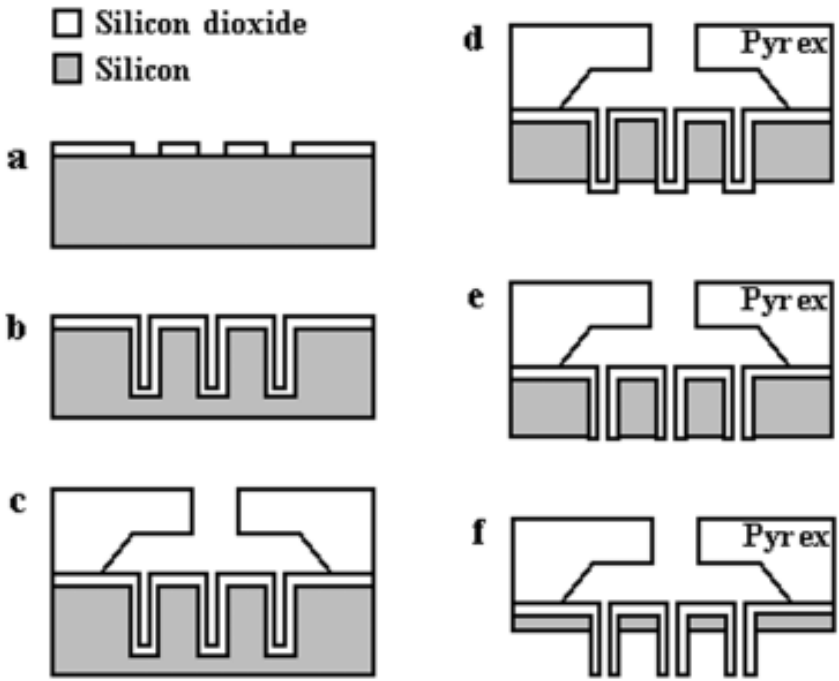

Figure 4 Hollow microcapillary fabrication sequence. (*a*) The patterned silicon wafer is deep reactive ion etched to form cylindrical holes partially through the wafer; (*b*) the silicon dioxide mask is removed and a second oxide layer is thermally grown; (*c*) a machined Pyrex substrate is anodically bonded to the oxide layer; (*d*) silicon opposite the Pyrex substrate is etched back with tetramethylammonium hydroxide to reveal the microcapillary tips; (*e*) the microcapillary tips are etched off in a hydrofluoric acid solution; and (*f*) the silicon is etched back further in tetramethylammonium hydroxide. This last etch defines the microcapillary heights. Adapted from Reference 39. This process yields microcapillaries shown in Figure 3.

wafer by deep reactive ion etching in an inductively coupled plasma-reactive ion etcher (Figure 4*a*). The oxide layer is removed, and a second oxide is grown (Figure 4*b*). The thickness of this second oxide layer defines the wall thickness of the capillary tubes. The wafer is then anodically bonded to a Pyrex glass substrate that has a reservoir machined into it (Figure 4*c*). The silicon opposite the Pyrex chamber is wet etched in a tetramethylammonium hydroxide solution (42) until the tips of the silicon dioxide microcapillaries are exposed (Figure 4*d*). The tips are then etched off (opening up the capillary tips) in a buffered hydrofluoric acid solution (Figure 4*e*), and the silicon is etched again with tetramethylammonium hydroxide (Figure 4*f*). The height of the microcapillaries is controlled by the length of this last wet etch.

The fabricated microcapillaries (Figure 3) were 30 μm in height and had a diameter of 5 μm. The capillaries have been used to inject a fluorescent dye

(4′,6-diamidino-2-phenylindole) into tobacco (BY-2) cell conglomerates (39). The cell conglomerates were placed onto a glass slide, the microcapillaries were then inserted into the cells, and the dye was injected into the cells by applying pressure with a syringe-like apparatus. The cells were then examined with a fluorescent microscope. Cells injected with dye were indeed fluorescent, whereas the two control cell populations (microcapillary insertion without dye or dye alone) did not exhibit intracellular fluorescence. The microcapillaries have also been used to inject a plasmid vector containing a gene encoding for β-glucuronidase into tobacco cell conglomerates (40). The tobacco cells exhibited a positive transient response (blue precipitate), and the two control cell populations (microcapillary insertion without DNA or DNA alone) did not. No damage to the microcapillaries was observed after insertion into cells.

Summary

To deliver DNA and other molecules into cells, dense arrays of both solid and hollow microneedles have been fabricated and demonstrated for laboratory applications. Arrays of very sharp pyramidal microprobes that are fabricated by a simple wet-etching process delivered genetic material into plant (tobacco leaves), nematode, and mammalian cells (rat smooth muscle cells). Arrays of hollow microcapillaries fabricated by a more complex, deep reactive ion etching process delivered genetic material into tobacco cells. Although solid microprobes are simpler to make, hollow microcapillaries have the potential to deliver material more precisely by injection through well-defined microcapillary lumens. However, because the currently designed microcapillaries do not taper to a sharp tip, treatment of bacteria, viruses, and other small targets may be difficult.

LOCAL TISSUE DELIVERY

Conventional drug delivery often involves administering medication systemically, thereby treating the desired region of the body, but also exposing other parts of the body to the drug, which can have detrimental effects. Drug delivery targeted to a precise region or tissue in the body can reduce side effects, minimize the dose of a costly drug, or provide a means of delivery to a location that is difficult to treat (43). Two novel devices for microinjecting drugs into neural and arterial tissue within the body are discussed below.

Microfabricated Probes for Injection into Neural Tissue

The field of neuroscience relies heavily on advancements in instrumentation that can enable communication directly with neurons. In addition to facilitating basic research, the ability to communicate with neurons is important for medical applications, such as the development of neural prostheses, which have the

potential to partially restore vision to the blind, hearing to the deaf, and control over limb, organ, and gland functions to the paralyzed (44). Recently, there has been great success with microprobes as electrical interfaces to neural systems, without significant tissue damage (26–32). Although electrical measurements assist our understanding of how neurons interact, there are other phenomena, such as complex biochemical reactions in cells, that also play a role in determining the functionality of neurons. Therefore, a device that can deliver very small and precise amounts of bioactive compounds into highly localized areas of neural tissue would be valuable. A multichannel silicon probe has been microfabricated to deliver such compounds into neural tissue while simultaneously recording electrical signals from neurons and electrically stimulating neurons in vivo (45, 46). Neural probes with 1–4 microchannels for drug delivery are shown in Figure 5.

The multichannel neural probes are bulk silicon micromachined, using a series of oxidation, boron diffusion, and wet-etching steps (45, 46; Figure 6). The neural probes are fabricated along with integrated complementary-metal-oxide-semiconductor (CMOS) circuitry and electrodes for neuron stimulation and recording, but only fabrication of the needle structure and microchannels is detailed here. The probes are made by first defining the microchannels. A silicon wafer with a

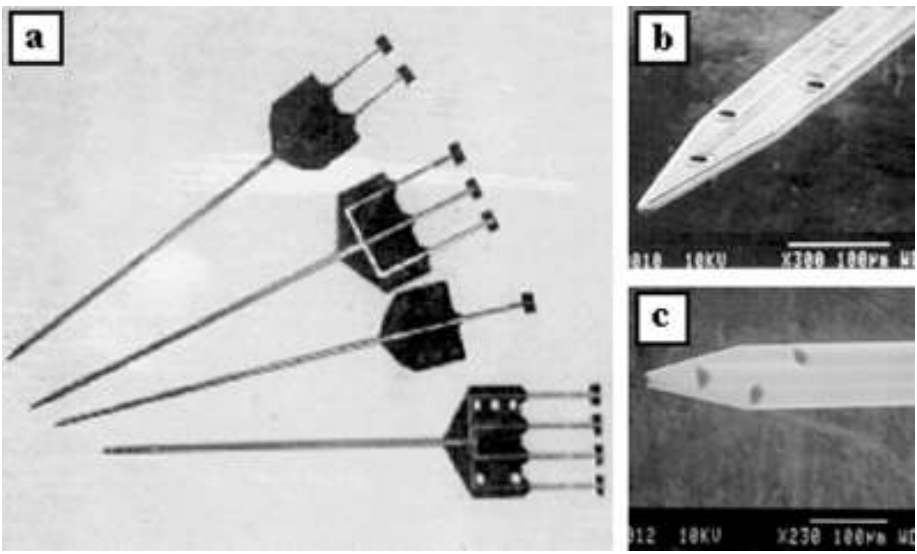

Figure 5 Scanning electron micrographs of (*a*) microfabricated neural probes with one to four microchannels, along with close-up views of the (*b*) top and (*c*) underside of a probe with three microchannels. These probes have been used to inject kainic acid and γ-aminobutyric acid into neural tissue while simultaneously stimulating and recording neuron activity. Reproduced with permission from Reference 46.

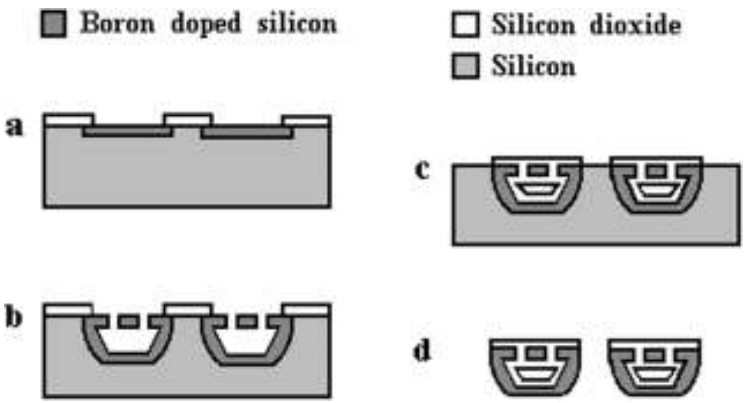

Figure 6 Neural probe fabrication sequence. A silicon wafer (*a*) with a patterned oxide layer is subjected to boron diffusion; (*b*) the boron layer is then patterned, anisotropically etched with EDP, and subjected to a second boron diffusion; (*c*) the openings in the top boron-doped layer are sealed by using thermal oxidation and low-pressure chemical vapor deposition of dielectrics; and (*d*) the wafer is then thinned from the backside with an isotropic etch, and the needles are released with an EDP etch. Adapted from Reference 46. This process yields microfabricated neural probes shown in Figure 5.

patterned silicon dioxide layer is subjected to boron diffusion [$<3\ \mu$m (Figure 6*a*)]. The boron layer is then photolithographically patterned, and the microchannels are anisotropically etched in an ethylenediaminepyrocatechol (EDP) solution (38, 47; Figure 6*b*). A second boron diffusion (7.5 μm) is performed to define the sides and the underside of the microprobe. The openings in the top layer of boron-doped silicon are then sealed by using thermal oxidation and low-pressure chemical vapor deposition of dielectrics (Figure 6*c*). Finally, the wafer is thinned from the backside with an isotropic wet etch, and the individual devices are released with an EDP etch (Figure 6*d*).

Fabricated probes were 4 mm in length, with 58- to 74-μm-wide shanks (46; Figure 5). The microchannels were 10–32 μm wide and 15 μm deep. To deliver precise amounts of bioactive compounds into neural tissue, it is important to determine the pressure needed to deliver a given amount of fluid. Of interest are volumes of $\sim$10–100 pl; it was determined experimentally that a 100-ms pulse of nitrogen at 10 lb/in^2 flowed 87 pl of distilled water through needles similar to those shown in Figure 5.

Multichannel neural probes were inserted and able to deliver both kainic acid (a neural stimulant) and γ-aminobutyric acid (a neural depressant) into guinea pig brains in vivo with minimal tissue disruption (46). Guinea pigs were anesthetized, and the skull bone and occipital cortex were removed to expose the superior colliculus and inferior colliculus. Neural probes were inserted into tissue, and a solution of kainic acid or γ-aminobutyric acid was injected. This resulted in either increased

or decreased neuronal activity, depending on the solution injected and the tissue treated.

Silicon Microprobes for Intravascular Drug Delivery

Although current methods to treat stenotic coronary arteries (e.g. balloon angioplasty, atherectomy, and coronary stenting) have great initial success in widening constricted arteries, up to one third of those treated suffer from restenosis within 6 months of treatment (48). The effectiveness of antirestenosis drugs given to prevent reblockage of arteries has been hindered by difficulties associated with delivering these drugs across arterial plaque. To provide a conduit across this barrier, microprobes similar to the pyramidal arrays described above (Figure 1) have been used to transect the internal elastic lamina (IEL) of normal and atherosclerotic rabbit arteries in vitro (37). This approach could be used to develop a coronary stent with micromechanical probes around its perimeter for piercing compressed plaque and delivering antirestenosis therapies into the arterial wall.

These silicon microprobes (Figure 1) were fabricated with bulk silicon micromachining as described above (35; Figure 2). Microprobes of different lengths were inserted into rabbit iliac arteries in vitro with applied pressures of 100, 300, and 500 mm Hg (37). These pressures are representative of intraluminal pressures measured during clinical stent deployment. Microprobes of 65 μm in length were not able to pierce through the IEL at any of the pressures tested. The IEL deformed around the microprobe instead of being pierced, even though the microprobe was very sharp (tip radius of curvature <0.1 μm). Microprobes of 140 μm in length pierced the IEL at an insertion pressure of 100 mm Hg and transected the IEL, media, and external elastic lamina and sometimes pierced the adventia when inserted with a pressure of 500 mm Hg. In atherosclerotic vessels, the 140-μm probes applied at 500 mm Hg could also transect the IEL, but only if the arterial plaque was sufficiently thin.

Summary

Two novel devices have been discussed that deliver drugs to specific target regions of tissue inside the body. Microfabricated neural probes have been used to deliver drugs into neural tissue of guinea pigs in vivo, while simultaneously monitoring and stimulating neuronal activity. Although the addition of microchannels to these devices requires only minor process changes, fabrication of the complete electrically active device is complex owing to its high level of functionality. Microprobes have also been inserted across vessel walls of normal and atherosclerotic rabbit arteries in vitro. Although the simplicity of the current fabrication technique is attractive, the use of anodic films to fabricate high-aspect-ratio molds for electrodeposition or injection molding is being investigated (49, 50) to increase needle density and permit nonplanar geometries.

SYSTEMIC DELIVERY

In recent years, biotechnology has produced a battery of sophisticated and potent drugs. However, methods to effectively deliver these drugs into the body have limitations (51–54). Oral delivery of these new protein-based, DNA-based, and other therapeutic compounds is generally not possible owing to drug degradation in the gastrointestinal tract and/or elimination by the liver. The usual alternative to oral delivery is via injection, either directly into the bloodstream or into tissues (e.g. subcutaneous or intramuscular injection). Although injection effectively delivers drug in large quantities, it has significant limitations, such as pain and tissue trauma caused by the needle, failure to provide convenient controlled or sustained release, and the need for expertise to perform an injection. The three devices reviewed in this section decrease the diameter and insertion depth of hypodermic needles to overcome some of these limitations. In addition, the third device is also designed to deliver drugs transdermally by microfabricated three-dimensional arrays of microneedles in a patch-like conformation.

Silicon and Polysilicon Microhypodermic Needles for Injection

By decreasing the size of hypodermic needles, insertion pain and tissue trauma experienced by patients can be reduced. Also, the combination of these needles with micropumps and other devices can yield more sophisticated needles that can potentially deliver drugs in a more controlled manner. Based on this motivation, silicon microhypodermic needles were fabricated with a combination of bulk and surface micromachining techniques (55, 56; Figures 7 and 8). Microhypodermic needles were also fabricated from polysilicon, using a polysilicon micromolding technique referred to as polymolding (57; see Figure 9). This latter process has the potential to be much more economical because it permits reuse of silicon micromolds.

Silicon microhypodermic needles, in combination with resistive heaters for bubble-pumping elements and an IC-interface region, are fabricated by a seven-mask IC-compatible process (55, 56; Figure 8); only the fabrication of the bulk micromachined needle structure and the surface micromachined fluidic channels is detailed here. A silicon wafer with a thermally grown oxide layer is patterned to open up regions in the oxide. The open regions of silicon define the shape of the needles. The wafer is then boron doped (12 μm deep) in the regions unprotected by the oxide masking layer (Figure 8*a*). This heavily doped boron region makes up a portion of the needle shaft.

Next, the microchannels are surface micromachined. A sacrificial layer consisting of 8 μm of silicon dioxide is vapor deposited. The microchannels are patterned and etched in a buffered hydrofluoric acid solution (Figure 8*b*). The sidewalls and top of the microchannels are created by depositing 1 μm of nitride onto the wafer. The nitride layer is then patterned, and etch holes (not shown) are opened up by reactive ion etching. The sacrificial glass layer is then removed in a concentrated

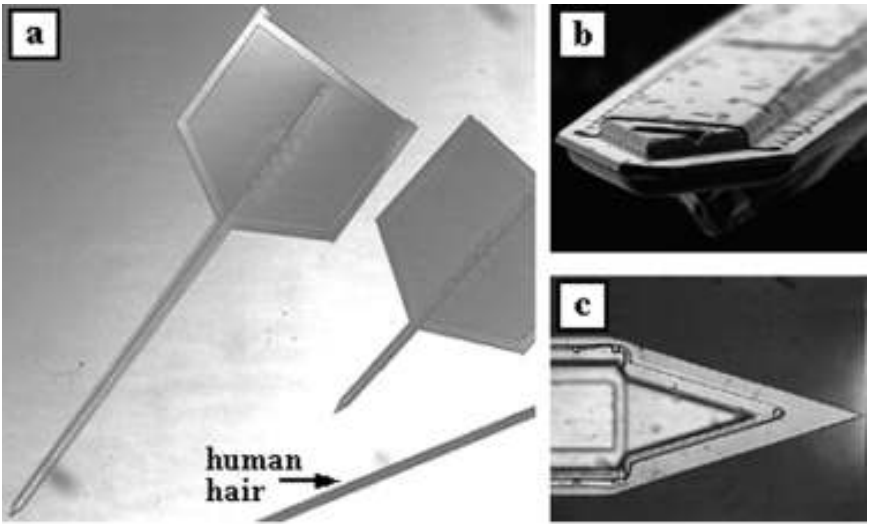

Figure 7 Scanning electron micrographs of (*a*) two silicon microhypodermic needles with different shaft lengths shown next to a human hair along with close-up views of the (*b*) front and (*c*) top of a microhypodermic needle tip. These needles were developed for injection across skin and have been coupled with bubble pumps and an integrated circuit interface region. Reproduced with permission from Reference 55.

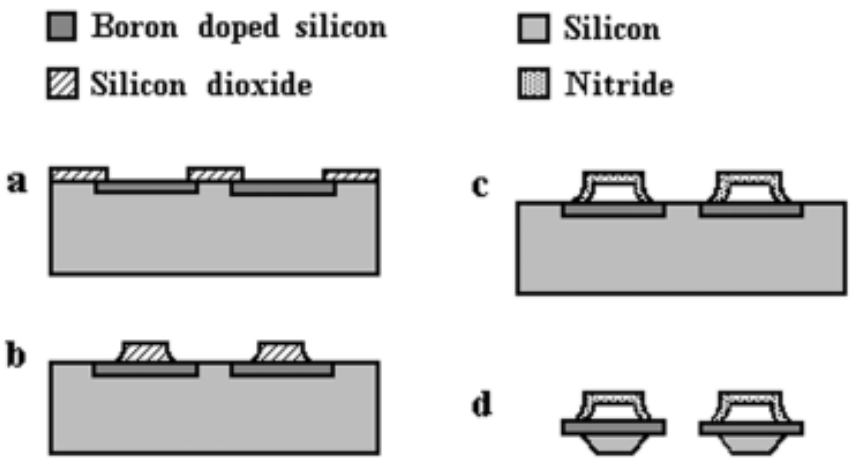

Figure 8 Silicon microhypodermic needle fabrication sequence. (*a*) A silicon wafer with a patterned oxide layer is subjected to boron diffusion to define a portion of the shank; (*b*) a sacrificial layer of oxide is deposited onto the wafer and patterned to define the microchannels; (*c*) a nitride layer is deposited to make the top and side walls of the needles, and the sacrificial oxide is removed; and (*d*) the needles are released from the silicon wafer with multiple EDP etches. Adapted from Reference 55. This process yields microhypodermic needles shown in Figure 7.

hydrofluoric acid solution, and the etch holes are sealed with the deposition of 1.5 μm of nitride (Figure 8*c*). The needles are released from the wafer with a series of wet EDP etches from the backside of the wafer (Figure 8*d*). About 50 μm of undoped silicon is left on the underside of the shank (except near the tip), which is left behind after the EDP release etches. This layer serves as added structural support for the shank of the needle.

The polymolding process uses two silicon wafers to micromold polysilicon microhypodermic needles (57; see Figure 10). To create the reusable silicon mold, two masks are required. The first mask defines holes to be etched through the top wafer of the mold (seen most clearly in Figure 9), and the second mask defines the overall needle geometry on the bottom half of the mold. The needle geometry is then deep reactive ion etched 100–130 μm into the silicon wafer (Figure 10*a*, which shows only the bottom half of the mold). A release layer (2–3 μm of

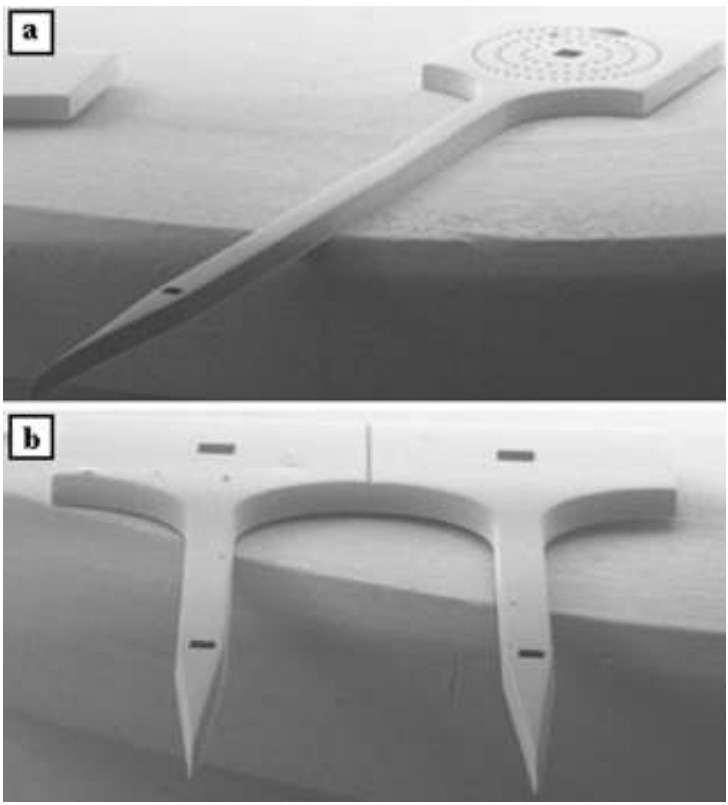

Figure 9 Scanning electron micrographs of (*a*) a single polysilicon microhypodermic needle and (*b*) a dual microhypodermic needle design developed for drug injection across the skin. Reproduced with permission from Reference 57.

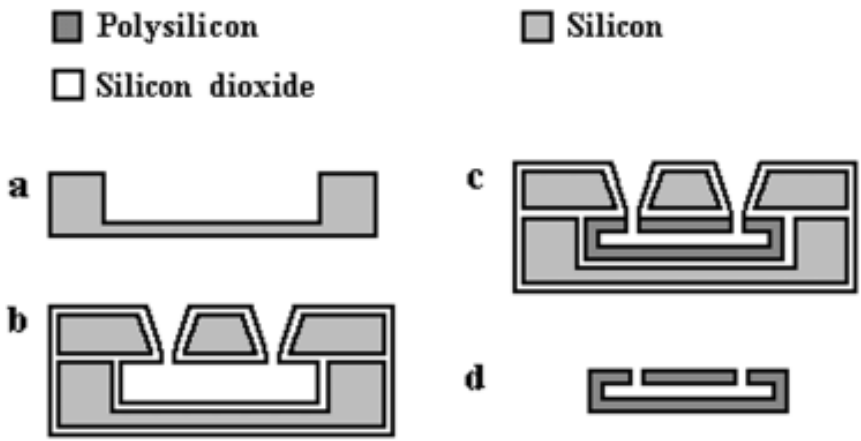

Figure 10 Polysilicon microhypodermic needle fabrication sequence. (*a*) The bottom wafer is patterned and deep reactive ion etched to define needle geometry; (*b*) an oxide release layer is deposited onto the bottom and top portions of the silicon mold, and the two portions are then pressure bonded together; (*c*) polysilicon is deposited to coat the inner walls of the silicon mold; and (*d*) the needles are released from the mold by etching away the oxide release layer. Adapted from Reference 57. This process yields microhypodermic needles shown in Figure 9.

silicon dioxide) is then deposited onto the top and bottom halves of the silicon mold. The two wafers are aligned and pressure bonded (Figure 10*b*). Low-pressure chemical vapor deposition polysilicon (3 μm) is uniformly deposited onto the mold. The polysilicon is then annealed in a high-temperature nitrogen atmosphere. This polysilicon deposition and the subsequent annealing process are repeated until 12–18 μm of polysilicon completely lines the interior and top of the mold. The polysilicon deposited on top of the mold is removed by deep reactive ion etching (Figure 10*c*). Finally, the polysilicon microhypodermic needles are released from the mold by etching the oxide release layer in a solution of hydrofluoric acid (Figure 10*d*).

The resulting silicon microhypodermic needles varied in length from 1 to 6 mm, their shanks were 140 μm wide, and they tapered to 80 μm toward the tip before coming to a sharp point (Figure 7). The surface-micromachined fluid channels were 50 μm wide and 9 μm deep, and they ran the full length of the needle. The port for fluid delivery or sampling was located 150 μm from the needle tip on the side of the needle and was 30 by 30 μm square. The silicon microhypodermic needles have been inserted into pieces of meat without bending or breaking (55, 56).

The polysilicon microhypodermic needles were 1–6 mm in length, measured 100–200 μm in diameter, and had tips with submicrometer radii in one dimension (Figure 9). With a wall thickness of 12 μm, the polysilicon needles were too weak to handle, but with 18-μm-thick walls, they were much stronger (57).

When reinforced with a thin coat of nickel, the needles were able to withstand bending moments of ≤0.71 milliNewton meter (mNm). Different polysilicon needle designs were also investigated, such as microneedles with dual shafts, internal reinforcements, or filters at their bases.

Metal Microhypodermic Needles for Injection

Microhypodermic needles have been fabricated from metal by surface micromachining techniques. Two designs have been investigated—a fluid-coupled, multiple-needle design (58; Figure 11) and a single-needle design with multiple output ports (59; Figure 12). The multiple-needle design limits penetration depth into the skin by the distance between its structural supports and the needle tips. These structural supports are hollow and in fluid communication with the needles, so they divert flow from clogged needles into neighboring unclogged needles. The multiple-output-port needle is also designed to divert flow if one or more of the ports become blocked.

The multiple-needle design and the multiple-output-port needles are fabricated similarly (58, 59; Figure 13). Palladium is selectively electroplated onto a silicon wafer to form the undersides of the needles (Figure 13*a*). A thick sacrificial layer of photoresist is deposited and patterned to define the inner dimensions of the hollow needles (Figure 13*b*). A seed layer is sputter deposited onto the wafer

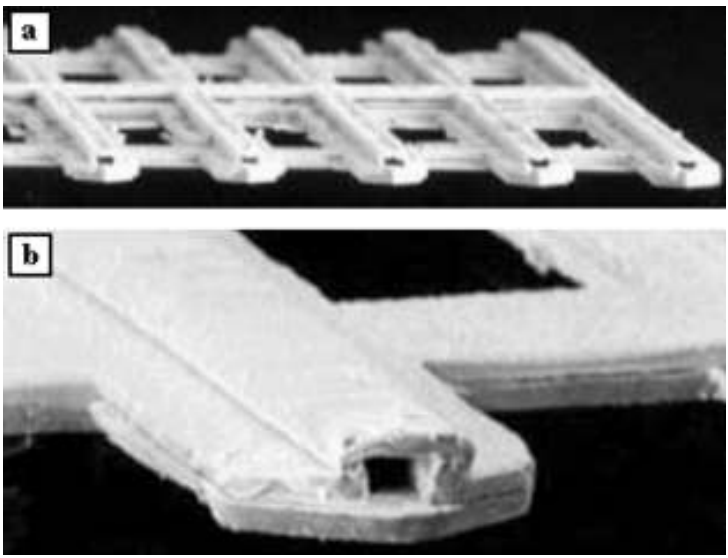

Figure 11 Scanning electron micrographs of (*a*) a fluid-coupled microhypodermic needle array and (*b*) a close-up view of a needle tip. These arrays of metal needles were developed for injection across skin; the hollow structural supports were designed to provide strength and redirect fluid from clogged needle tips. Reproduced with permission from Reference 58.

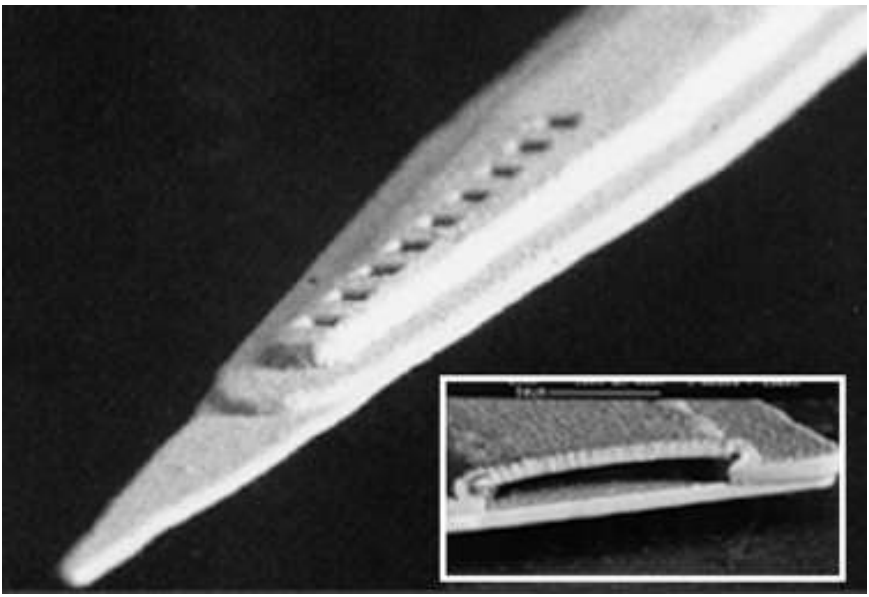

Figure 12 Scanning electron micrograph of a metal needle with multiple output ports and a cross-section of the needle showing its microchannel (*insert*). The multiple ports were designed to reduce the effects of port clogging. Reproduced with permission from Reference 59.

to uniformly coat the sacrificial photoresist layer. A layer of palladium is then electroplated onto the seed layer to form the sidewalls and top surfaces of the needles. The sacrificial photoresist is removed by soaking the wafer in acetone (Figure 13*c*). The structures are finally released by etching away the underlying seed layer (Figure 13*d*). The multiple-output-port needle can be packaged in a standard luer-lock fitting. Needles have also been fabricated from gold and nickel.

The fluid-coupled needles were fabricated as 25-needle linear arrays with a 200-μm center-to-center spacing (Figure 11). Their flow channels were 20 μm by 40 μm with a wall thickness of 20 μm. The distance between the needle tips and the structural supports was 250 μm. Pressure drops of 0.15–1.6 lb/in^2 across 3-mm-long channels (600 μm by 30 μm each) yielded water flow rates of 50–650 μl/min (58). Although not demonstrated, these needles have been proposed both as microhypodermic needles and for sustained transdermal drug delivery, as discussed below.

The multiple-output-port needles were 6 mm in length, had tip dimensions of $<$15 μm by 15 μm, channel dimensions of 140 μm by 20 μm, shaft dimensions of 200 μm by 60 μm, and a distance from tip to first output port of 300 μm (Figure 12). Pressure drops of 1–70 lb/in^2 across a 6-mm-long channel (140 μm by 20 μm) with multiple ports (30 μm by 30 μm) yielded water flow rates of 0.004–2.7 μl/min (59).

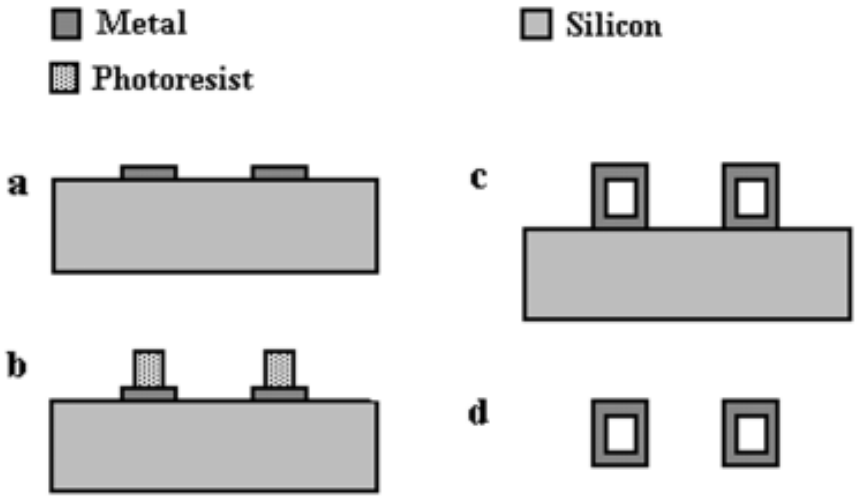

Figure 13 Metal microhypodermic needle fabrication sequence. (*a*) The undersides of the metal needles are selectively electroplated onto the surface of the silicon substrate; (*b*) a thick sacrificial layer of photoresist is deposited and patterned to define the microchannels; (*c*) a seed layer is sputter deposited onto the sacrificial photoresist, and the top and side walls of the microneedles are electroplated; and (*d*) the sacrificial photoresist is removed and the needles are released from the substrate. Adapted from Reference 59. This process yields needles shown in Figures 11 and 12.

Microneedles for Transdermal Drug Delivery

As opposed to short-term delivery by injection, transdermal delivery of drugs over extended periods of time (e.g. up to days) is a convenient, controlled way to administer medication, as shown by recent success with nicotine and other patches (60). However, conventional (microneedle-free) transdermal drug delivery, which relies on drugs passively diffusing across the skin, is severely hindered by the extraordinary barrier properties of the outer 10–20 μm of skin, the stratum corneum (61, 62). Because the stratum corneum contains no nerves, the development of microneedles that are long and robust enough to penetrate across this layer, but short enough not to stimulate nerves in deeper tissues, has the potential to make transdermal delivery of many more drugs possible. As a first-generation microneedle-based transdermal patch, arrays of bulk micromachined solid silicon microneedles were fabricated and shown to increase skin permeability to a variety of different molecules by orders of magnitude, including macromolecules (63, 64; Figure 14*b* and *c*). As an improved design, arrays of hollow silicon (not shown) and hollow metal microneedles (Figure 14*d* and *e*) were fabricated that increased skin permeability still further (65, 66).

Arrays of solid silicon microneedles are fabricated by a single-mask process that defines arrays of chromium circles on a silicon wafer (63, 64; Figure 2*a–c*).

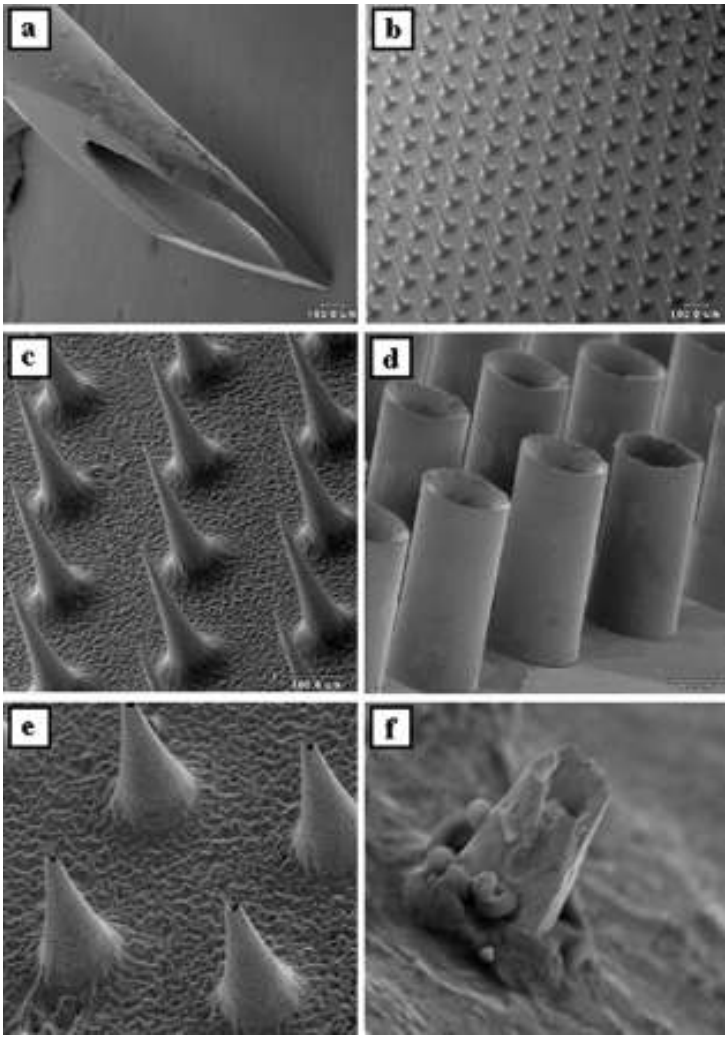

Figure 14 Scanning electron micrographs of (*a*) a 26-gauge hypodermic needle, (*b*) a silicon microneedle array shown at the same magnification as the hypodermic needle and (*c*) at higher magnification, (*d*) a hollow metal microtube array, (*e*) a hollow metal microneedle array, and (*f*) a tip of a hollow metal microneedle penetrating up through the underside of human epidermis. These microneedle arrays have been shown to penetrate skin without breaking, increase skin permeability up to 100,000-fold, and not cause pain in human subjects. Reproduced with permission from References 65 and 66.

The wafer is then anisotropically etched by a modification of the black silicon method (67) in a reactive ion etcher (Figure 2*d*). The needles are etched until the chromium masks are undercut and fall off, leaving behind arrays of microneedles (Figure 14*b* and *c*). Hollow silicon microneedles have also been fabricated by using deep reactive ion etching in an inductively coupled reactive ion etcher (65). This deep etch creates arrays of holes through the silicon wafer (each hole defines a microneedle lumen), and the tapered walls of the microneedles are formed by reactive ion etching around these holes, as described above for solid silicon needles.

Arrays of hollow metal microtubes (Figure 14*d*) and microneedles (Figure 14*e* and *f*) are fabricated by defining molds in epoxy and filling them by electrodepositing metal (65, 66; Figure 15). A thick layer of UV-light–photosensitive epoxy (SU-8) is coated onto a silicon or glass substrate (Figure 15*a*). To make microtubes, the epoxy mold is photodefined to create vertical walled holes, which define the microtube geometry (Figure 15*b*). For microneedles, the tapered wall holes are defined in the mold by casting the epoxy over an array of solid-silicon microneedles (not shown). A conductive seed layer is then uniformly sputter deposited onto the epoxy molds, and metal is electroplated to partially fill the mold (Figure 15*c*). The mold is then etched away leaving behind an array of hollow tubes (Figure 14*d*) or conical shells [i.e. hollow microneedles (Figure 14*e*)].

Arrays of solid silicon microneedles were fabricated with individual needles measuring 150 μm tall, 80 μm in diameter at their base, and tapering to sharp tips

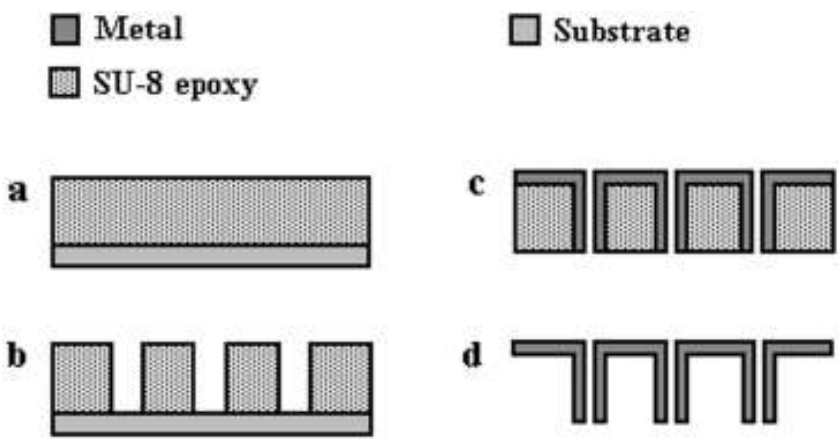

Figure 15 Hollow metal microneedle and microtube fabrication sequence. (*a*) SU-8 photosensitive epoxy is spin cast onto a substrate; (*b*) cylindrical holes are photodefined into the epoxy (microtubes as shown), or conical holes are made in the epoxy by molding solid needles (microneedles—not shown); (*c*) a seed layer is deposited, and a layer of metal is electroplated onto the epoxy molds; and (*d*) the hollow metal microneedles or microtubes are released from the epoxy molds. Adapted from Reference 65. This process yields hollow microneedles shown in Figure 14*d* and *e*.

with radii of curvature of <1 μm (Figure 14*c*). Needles had a center-to-center spacing of 150 μm and were arranged in a 20 by 20 array (i.e. 400 needles). Figures 14*a* and *b* show a 26-gauge hypodermic needle and a portion of a microneedle array at the same magnification. Hollow microneedles and microtubes were fabricated with similar dimensions to the solid microneedles, except that they contained hollow bores of 5–70 μm in diameter, depending on needle design (Figure 14*d* and *e*).

Solid microneedles could be inserted into human epidermis (the outer ~100 μm of skin, including the stratum corneum) with ~10 N of force for a 400-needle array, without damaging the needles (64). These needle arrays were then used to transport molecules across human epidermis in vitro, either with the needles remaining embedded in the skin or after they were removed. Transport of three molecules has been investigated: calcein (623 Daltons; represents small impermeant drugs), insulin (5800 Daltons), and bovine serum albumin (66,000 Daltons; represents large proteins). Skin permeability to these three molecules was increased ≤10,000-fold above the sensitivity limit of the assay equipment [10^{-6} cm/h (66)]. Companion studies conducted in humans showed that subjects reported that microneedles were painless. Hollow microneedles have also been inserted into human epidermis without breaking (Figure 14*f*) and were shown to increase skin permeability ≤100,000-fold above the assay sensitivity limit (66).

Summary

To reduce pain and tissue trauma and to provide better control over drug delivery, a number of microneedle designs have been developed. Silicon microhypodermic needles have been fabricated in combination with heat-controlled bubble pumps. Using a more cost-effective technique, similar polysilicon microneedles have also been made with reusable molds. Metal microhypodermic needles have been fabricated and shown to flow water through their bores under modest applied pressures. For application to transdermal drug delivery, three-dimensional arrays of solid-silicon microneedles have been made that increased skin permeability ≤4 orders of magnitude in vitro and have been reported to be painless in human trials. Arrays of hollow silicon and metal microneedles have also been fabricated directly and from molds; they were shown to increase skin permeability ≤5 orders of magnitude in vitro. Microneedle designs based on reusable molds are likely to be most cost effective and thus have the potential to produce single-use disposable microneedles.

CONCLUSIONS

Microfabrication technology has made possible the creation of microscopic devices that can be used for a broad range of biological applications. One compelling application described here is microneedles, which have been fabricated by using a variety of microfabrication techniques and have been shown to deliver genes and drugs into cells, local regions of tissue, and across the skin. Optimal microneedle

designs appear to be those that are (*a*) hollow (rather than solid), because this permits better controlled delivery; (*b*) made out of materials other than the industry standard silicon because materials such as metal or polysilicon are less expensive, stronger, and/or proven to be biocompatible; and (*c*) manufactured by micromolding techniques (as opposed to conventional bulk or surface micromachining), because this approach is likely to be less expensive for mass production.

ACKNOWLEDGMENTS

We thank JD Brazzle, K Chun, L Lin, AP Pisano, ML Reed, and KD Wise for contributing digital images of their work for this paper. This work was supported in part by the National Science Foundation, American Diabetes Association, and the Defense Advanced Research Project Agency. MR Prausnitz and MG Allen have a significant financial interest in a company called Redeon, Inc., which is developing products related to this study. The terms of this arrangement have been reviewed and approved by Georgia Institute of Technology and Emory University in accordance with their conflict of interest policies.

LITERATURE CITED

1. The World Book Encyclopedia. 1999. Hypodermic injection. In *The World Book Encyclopedia*, 9:480–81. Chicago: World Book
2. Zehr L. 1999. *The End of the Needle*. http://www.globetechnology.com/archive/gam/News/19990520/TWORAL.html
3. Deleted in proof
4. Madou M. 1997. *Fundamentals of Microfabrication*. Boca Raton, FL: CRC Press. 589 pp.
5. Jaeger RC. 1988 *Introduction to Microelectronics Fabrication*. Reading, MA: Addison-Wesley. 232 pp.
6. Runyan WR, Bean KE. 1990. *Semiconductor Integrated Circuit Processing Technology*. Reading, MA: Addison-Wesley. 683 pp.
7. Gerstel MS, Place VA. 1976. *US Patent No. 3964482*
8. Leighton SB, Brownstein MJ. 1993. *US Patent No. 5262128*
9. Ginaven RO, Facciotti D. 1995. *US Patent No. 5457041*
10. Lin L, Pisano AP. 1997. *US Patent No. 5591139*
11. Godshall NA, Anderson RR. 1999. *US Patent No. 5879326*
12. System Plan. Corp. 1999. *MicroElectroMechanical Systems (MEMS): An SPC Market Study*. Arlington, VA: System Plan. Corp. 16 pp.
13. O'Donnell-Maloney MJ, Smith CL, Cantor CR. 1996. The development of microfabricated arrays for DNA sequencing and analysis. *Trends Biotechnol.* 14(10):401–7
14. Burke DT, Burns MA, Mastrangelo C. 1997. Microfabrication technologies for integrated nucleic acid analysis. *Genome Res.* 7(3):189–97
15. Mastrangelo CH, Burns MA, Burke DT. 1998. Microfabricated devices for genetic diagnostics. *Proc. IEEE* 86(8):1769–87
16. Dario P, Valleggi R, Carrozza MC, Montesi MC, Cocco M. 1992. Microactuators for microrobots: a critical survey. *J. Micromech. Microeng.* 2(3):141–57

17. Lim G, Park K, Sugihara M, Minami K, Esashi M. 1996. Future of active catheters. *Sens. Actuators A* 56(1–2):113–21
18. Lal A, White RM. 1995. Micromachined silicon needle for ultrasonic surgery. *IEEE Ultrasonics Symp., Seattle,* pp. 1593–96. Piscataway, NJ: IEEE
19. Lin G, Palmer RE, Pister KSJ, Roos KP. 1997. Single heart cell force measured in standard CMOS. *Transducers 97*, *Proc. Int. Conf. Solid-State Sens. Actuators, 11th, Chicago*, pp. 199–200. Piscataway, NJ: IEEE
20. Brody JP, Han YQ, Austin RH, Bitensky M. 1995. Deformation and flow of red blood cells in a synthetic lattice: evidence for an active cytoskeleton. *Biophys. J.* 68(6):2224–32
21. Wolf B, Brischwein M, Baumann W, Ehrey R, Kraus M. 1998. Monitoring of cellular signaling and metabolism with modular sensor-technique: the Physio-Control-Microsystem (PCM). *Biosens. Bioelectron.* 13(5):501–9
22. Akin T, Najafi K, Smoke RH, Bradley RM. 1994. A micromachined silicon sieve electrode for nerve regeneration applications. *IEEE Trans. Biomed. Eng.* 41(4):305–13
23. Santini JT, Cima MJ, Langer R. 1999. A controlled-release microchip. *Nature* 394(6717):335–38
24. Liu CC, Jin Z. 1997. Applications of microfabrication and micromachining techniques to biotechnology. *Trends Biotechnol.* 15(6):213–16
25. Voldman J, Gray ML, Schmidt MA. 1999. Microfabrication in biology and medicine. *Annu. Rev. Biomed. Eng.* 1:401–25
26. Wise KD, Angell JB, Starr A. 1970. An integrated circuit approach to extracellular microelectrodes. *IEEE Trans. Biomed. Eng.* 17(3):238–46
27. Najafi K, Wise KD, Mochizuki T. 1985. A high-yield IC-compatible multichannel recording array (neural activity probe). *IEEE Trans. Electron. Device* 32(7):1206–11
28. Drake KL, Wise KD, Farraye J, Anderson DJ, BeMent SL. 1988. Performance of planar multisite microprobes in recording extracellular single-unit intracortical activity. *IEEE Trans. Biomed. Eng.* 35(9):719–32
29. Campbell PK, Jones KE, Huber RJ, Horch KW, Normann RA. 1991. A silicon-based, three-dimensional neural interface: manufacturing processes for an intracortical electrode array. *IEEE Trans. Biomed. Eng.* 38(8):758–68
30. Carter RR, Houk JC. 1993. Multiple single-unit recordings from the CNS using thin-film electrode arrays. *IEEE Trans. Rehabil. Eng.* 1(3):175–84
31. Frazier AB, O'Brien DP, Allen MG. 1993. Two-dimensional metallic microelectrode arrays for extracellular stimulation and recording of neurons. *Proc. IEEE Micro Electro Mech. Syst. Workshop, 6th, Fort Lauderdale, FL*, pp. 195–200. Piscataway, NJ: IEEE
32. Bragin A, Jando G, Nadasdy Z, Hetke J, Wise K, Buzsaki G. 1995. Gamma (40 Hz–100 Hz) oscillation in the hippocampus of the behaving rat. *J. Neurosci.* 15(1):47–60
33. Celis JE. 1984. Microinjection of somatic cells with micropipettes: comparison with other transfer techniques. *Biochem. J.* 223(2):281–91
34. McNeil PL. 1989. Incorporation of macromolecules into living cells. *Methods Cell Biol.* 29:153–73
35. Trimmer W, Ling P, Chin CK, Orton P, Gaugler R, et al. 1995. Injection of DNA into plant and animal tissues with micromechanical piercing structures. *Proc. IEEE Micro Electro Mech. Syst. Workshop, 8th, Amsterdam*, pp. 111–15. Piscataway, NJ: IEEE
36. Hashmi S, Ling P, Hashmi G, Reed ML, Gaugler R, Trimmer W. 1995. Genetic transformation of nematodes using arrays of micromechanical piercing structures. *BioTechniques* 19(5):766–70
37. Reed ML, Clarence W, James K, Watkins S, Vorp DA, et al. 1998. Micromechanical

devices for intravascular drug delivery. *J. Pharm. Sci.* 87(11):1387–94
38. Seidel H, Csepregi L, Heuberger A, Baumgärtel H. 1990. Anisotropic etching of crystalline silicon in alkaline solutions. II. Influence of dopants. *J. Electrochem. Soc.* 137(11):3626–32
39. Chun K, Hashiguchi G, Toshiyoshi H, Le Pioufle B, Ishikawa J, et al. 1999. DNA injection into plant cell conglomerates by micromachined hollow microcapillary arrays. Proc. IEEE *Micro Electro Mech. Syst. Workshop, 12th, Orlando*, Piscataway, NJ: IEEE
40. Chun K, Hashiguchi G, Toshiyoshi H, Fujita H. 1999. Fabrication of array of hollow microcapillaries used for injection of genetic materials into animal/plant cells. *Jpn. J. Appl. Phys. Part 2* 38(3A):279–81
41. Chun K, Hashiguchi G, Toshiyoshi H, Fujita H, Kikuchi Y, et al. 1999. An array of hollow microcapillaries for the controlled injection of genetic materials into animal/plant cells. *Transducers 99, Int. Conf. Solid-State Sens. Actuators, 10th, Sendai*, pp. 44–47. Tokyo: IEE Jpn.
42. Tabata O, Asahi R, Funabashi H, Shimaoka K, Sugiyama S. 1992. Anisotropic etching of silicon in TMAH solutions. *Sens. Actuators A* 34(1):51–57
43. Langer R. 1998. Drug delivery and targeting. *Nature* 392(6679):5–10
44. Agnew WF, McCreery DB. 1990. *Neural Prostheses: Fundamental Studies*. Englewood Cliffs, NJ: Prentice Hall. 322 pp.
45. Chen J, Wise KD. 1994. A multichannel neural probe for selective chemical delivery at the cellular level. *Tech. Dig. IEEE Solid-State Sens. Actuator Workshop, Hilton Head Island, SC*, pp. 256–69. Cleveland Heights, OH: Transducers Res. Found.
46. Chen J, Wise KD. 1997. A multichannel neural probe for selective chemical delivery at the cellular level. *IEEE Trans. Biomed. Eng.* 44(8):760–69
47. Bassous E. 1978. Fabrication of novel three-dimensional microstructures by anisotropic etching of (100) and (110) silicon. *IEEE Trans. Electron Device* 25(10):1178–84
48. Serruys PW, Strauss BH, King SB. 1992. *Restenosis After Intervention with New Mechanical Devices*. Boston: Kluwer Acad. 504 pp.
49. Tan SS, Reed ML, Han H, Boudreau R. 1995. High aspect ratio microstructures on porous anodic aluminum oxide. *Proc. IEEE Micro Electro Mech. Syst. Workshop, 8th, Amsterdam*, pp. 267–72. Piscataway, NJ: IEEE
50. Nadeem A, Mescher M, Rebello K, Reed ML, Weiss L, Feldman M. 1998. Fabrication of microstructures using aluminum anodization techniques. *Proc. IEEE Micro Electro Mech. Syst. Workshop, 11th, Heidelberg*, pp. 274–77. Piscataway, NJ: IEEE
51. Langer R. 1990. New methods of drug delivery. *Science* 249:1527–33
52. Crystal RG. 1995. Transfer of genes to humans: early lessons and obstacles to success. *Science* 270:404–10
53. Amsden BG, Goosen MFA. 1995. Transdermal delivery of peptide and protein drugs: an overview. *AIChHE J.* 41(8): 1972–97
54. Shahrokh Z, Sluzky V, Cleland J, Shire S, Randolph T, eds. 1997. *Therapeutic Protein and Peptide Formulation and Delivery*. Washington, DC: Am. Chem. Soc. 228 pp.
55. Lin L, Pisano AP, Muller RS. 1993. Silicon processed microneedles. *Transducers 93, Int. Conf. Solid-State Sens. Actuators, 4th, Yokohama*, pp. 237–40. Tokyo: IEEE Jpn.
56. Lin L, Pisano AP. 1999. Silicon processed microneedles. *IEEE J. Micromech. Syst.* 8(1):78–84
57. Talbot NH, Pisano AP. 1998. Polymolding: two wafer polysilicon micromolding of closed-flow passages for microneedles and microfluidic devices. *Tech. Dig. IEEE Solid-State Sens. Actuator Workshop, Hilton Head Island, SC*, pp. 265–68.

Cleveland Heights, OH: Transducers Res. Found.
58. Brazzle JD, Papautsky I, Frazier AB. 1998. Fluid-coupled hollow metallic micromachined needle arrays. *Proc. SPIE Conf. Microfluidic Dev. Syst., Santa Clara, CA*. 3515:116–24
59. Brazzle JD, Mohanty S, Frazier AB. 1999. Hollow metallic micromachined needles with multiple output ports. *Proc. SPIE Conf. Microfluidic Dev. Syst., Santa Clara, CA*. 3877(35):257–66
60. Guy RH. 1996. Current status and future prospects of transdermal drug delivery. *Pharm. Res.* 13(2):1765–69
61. Holbrook KA, Odland GF. 1974. Regional differences in the thickness (cell layers) of the human stratum corneum: an ultrastructural analysis. *J. Invest. Dermatol.* 62(4):415–22
62. Champion RH, Burton JL, Ebling FJG, eds. 1992. *Textbook of Dermatology*. London: Blackwell Sci. 3160 pp.
63. Henry S, McAllister DV, Allen MG, Prausnitz MR. 1998. Micromachined needles for the transdermal delivery of drugs. *Proc. IEEE Micro Electro Mech. Syst. Workshop, 11th, Heidelberg*, pp. 494–98. Piscataway, NJ: Inst. Electr. Electronics Eng.
64. Henry S, McAllister DV, Allen MG, Prausnitz MR, 1998. Microfabricated microneedles: a novel approach to transdermal drug delivery. *J. Pharm. Sci.* 87(8):922–25
65. McAllister DV, Cros F, Davis SP, Matta LM, Prausnitz MR, Allen MG. 1999. Three-dimensional hollow microneedle and microtube arrays. *Transducers 99, Int. Conf. Solid-State Sens. Actuators, 10th, Sendai*, pp. 1098–101. Tokyo: IEEE
66. McAllister DV, Kaushik S, Patel PN, Mayberry JL, Allen MG, Prausnitz MR. 1999. Solid and hollow microneedles for transdermal drug delivery. *Proc. Int. Symp. Control. Release Bioact. Mater., 26th, Boston*, pp. 192–93. Deerfield, IL: Control. Release Soc.
67. Jansen H, de Boer M, Otter B, Elwenspoek M. 1995. The black silicon method IV: the fabrication of three-dimensional structures in silicon with high aspect ratios for scanning probe microscopy and other applications. *Proc. IEEE Micro Electro Mech. Syst. Workshop, 8th, Amsterdam*, pp. 88–93. Piscataway, NJ: IEEE